Thermodynamics of Denaturant-Induced Unfolding of a Protein That Exhibits Variable Two-State Denaturation†

Allan Chris M. Ferreon and D. W. Bolen*

Department of Human Biological Chemistry and Genetics, Sealy Center for Structural Biology, University of Texas Medical Branch, 301 University Boulevard, 5.154 Medical Research Building, Galveston, Texas 77555

Received June 25, 2004; Revised Manuscript Received August 13, 2004

ABSTRACT: Free energy changes ($\Delta G^{\circ}_{N\rightarrow D}$) obtained by denaturant-induced unfolding using the linear extrapolation method (LEM) are presumed to reflect the stability differences between native (N) and denatured (D) species in the absence of denaturant. It has been shown that with urea and guanidine hydrochloride (GdnHCl) some proteins exhibit denaturant-independent $\Delta G^{\circ}_{N\rightarrow D}$. But with several other proteins urea and GdnHCl give different $\Delta G^{\circ}_{N\rightarrow D}$ values for the same protein, meaning that the free energy difference between N and D is not the only contribution to one or both $\Delta G^{\circ}_{N\rightarrow D}$ values. Using β1, a mutant form of the protein G B1 domain, we show that both urea- and GdnHCl-induced denaturations are two-state and reversible but that the denaturants give different values for $\Delta G^{\circ}_{N\rightarrow D}$. While spectral observables are sensitive to the shift between N and D states (between states effect), they are not sensitive to denaturant-induced changes that occur within the individual N and D states (within state effect). By contrast, nonspectral observables such as Stokes radius and thermodynamic observables such as proton uptake/release are often sensitive to both "between states" and "within state" effects. These observables, along with spectral measurements, provide descriptions of urea- and GdnHCl-induced denaturation of β1. Our results suggest that in the predenaturation concentration range GdnHCl changes the free energy of the native ensemble in a nonlinear manner but that urea does not. As with RNase A and β-lactoglobulin, β1 exhibits *variable two-state* behavior with GdnHCl-induced denaturation in that the free energy of the native ensemble in the predenaturation zone changes (varies) with GdnHCl concentration in a nonlinear manner.

In the field of protein folding, the linear extrapolation method (LEM)[1] is a frequently used procedure for obtaining the difference in stability between the native (N) and denatured (D) states of a protein (*1*−*3*). Protein stability is expressed as a free energy change ($\Delta G^{\circ}_{N\rightarrow D}$) obtained upon linear extrapolation of cooperative unfolding free energy data to zero denaturant concentration, where $\Delta G^{\circ}_{N\rightarrow D}$ is said to represent the free energy difference between N and D species in the absence of denaturant. More often than not, with many proteins, $\Delta G^{\circ}_{N\rightarrow D}$ values obtained for the same protein using urea and guanidine hydrochloride (GdnHCl) are found to be different (*4*−*8*), and this raises serious questions about the interpretation of this most basic description of protein stability.

To gain insight into the origins of $\Delta G^{\circ}_{N\rightarrow D}$ differences obtained using urea and GdnHCl, it is useful to consider the LEM and how a linear free energy relationship between native and denatured protein might arise. As shown by Greene and Pace, cooperative two-state denaturation empirically shows that the free energy difference ($\Delta G = G_D - G_N$) between the native (G_N) and denatured (G_D) states is a linear function of denaturant concentration (*1*). A simple way for ΔG to be a linear function of denaturant concentration would be for the respective free energies of the native and denatured states (G_N and G_D) to also be linear functions of denaturant concentration. In such a case, a plot of G_N and G_D versus denaturant concentration will result in two intersecting straight lines of negative slope. The difference between the two lines at each denaturant concentration gives ΔG as a linear function of denaturant concentration, and the intersection point defines $C_{1/2}$, the denaturant concentration at the midpoint of the N ↔ D transition.

The concept of the individual free energies of native and denatured states being linear functions of denaturant concentration provides a plausible explanation of underlying phenomena leading to the LEM. Assuming that linearity of G_N and G_D with denaturant concentration constitutes the basic principles behind the LEM, the question is whether deviations from these linear relationships are responsible for the lack of agreement in $\Delta G^{\circ}_{N\rightarrow D}$ often observed for urea- and GdnHCl-induced denaturation (*2*, *4*). An answer to this question should provide insight into why GdnHCl- and urea-derived $\Delta G^{\circ}_{N\rightarrow D}$ values differ for a number of proteins and what actual molecular processes these values describe.

In previous studies, we defined three classes of proteins based on their thermodynamic responses to urea and GdnHCl (*8*). By thermodynamic responses, we mean that denaturants

† Support provided by NIGMS-60292. A.C.M.F. is the recipient of the Sealy Center for Structural Biology predoctoral fellowship.

* To whom correspondence and reprint requests should be sent. Telephone: (409) 772-0754. Fax: (409) 772-1790. E-mail: dwbolen@utmb.edu.

[1] Abbreviations: β1, T2Q I6A T44A protein G B1 domain; $\Delta G^{\circ}_{N\rightarrow D}$, free energy change of unfolding; LEM, linear extrapolation method; GdnHCl, guanidine hydrochloride; $\Delta\nu$, proton uptake or release; SEC, size exclusion chromatography; K_d, partition coefficient; DLS, dynamic light scattering; DSC, differential scanning calorimetry.

10.1021/bi048666j CCC: $27.50
Published on Web 09/30/2004

affect the thermodynamics of N and D in more than one way. Denaturants most certainly shift the N ↔ D equilibrium, but they can also change the thermodynamic behavior of the individual N and D ensembles nonlinearly with denaturant concentration. The three classifications of proteins are based on whether the thermodynamic behavior of the N and/or D ensembles becomes nonlinear with respect to denaturant concentration and, if so, whether such changes take place within the cooperative transition zone or outside the transition zone.

The three classifications are important in interpreting $\Delta G^{\circ}_{N\rightarrow D}$ values obtained using the LEM. The first of the three classes of proteins exhibits no evidence of their N or D ensembles being anything other than linearly dependent on urea or GdnHCl concentration. The denaturant-induced unfolding of this class of protein is said to exhibit *fixed two-state behavior*, and the $\Delta G^{\circ}_{N\rightarrow D}$ values obtained via the LEM using urea and GdnHCl are found to be identical (*8*). For this class of proteins, $\Delta G^{\circ}_{N\rightarrow D}$ is a property of the protein alone and can be interpreted solely in terms of the N ↔ D equilibrium. Fixed two-state behavior is what most everyone trusts their particular protein exhibits.

At denaturant concentrations in the range preceding the spectrally observed onset of the cooperative transition, GdnHCl is often found to alter the thermodynamic behavior of the N state ensemble, and proteins that exhibit this behavior comprise a second class of protein denaturations (*8*). This effect of GdnHCl on the native state ensemble results in different values for $\Delta G^{\circ}_{N\rightarrow D}$ determined from urea- and GdnHCl-induced denaturation measurements. The thermodynamic consequence of this GdnHCl effect on the N ensemble is that the $\Delta G^{\circ}_{N\rightarrow D}$ obtained via the LEM contains free energy contributions not only from the shift between N and D species but also as a result of GdnHCl's specific action on the N state. By specific action on the N state we mean that at zero GdnHCl concentration the principal species is N, but with addition of GdnHCl in the pretransition range the N state is converted to N*, a structurally similar but thermodynamically distinct species. So long as the effect of GdnHCl on converting N → N* is completed before the onset of the denaturation transition, the $\Delta G^{\circ}_{N\rightarrow D}$ value obtained from the LEM is interpretable in terms of the equilibrium N* ↔ D. For this class of protein denaturations, GdnHCl is said to induce *variable thermodynamic character in the native ensemble outside the transition zone*. This effect causes differences in $\Delta G^{\circ}_{N\rightarrow D}$ values obtained from urea- and GdnHCl-induced denaturation of proteins (*8*).

In contrast to GdnHCl, in the limited number of cases we have investigated, the free energies of N or D ensembles always exhibit a linear dependence on urea concentration (*8*). Consequently, with this second class of proteins, the $\Delta G^{\circ}_{N\rightarrow D}$ obtained from urea-induced denaturation is presumed to be a property solely of the protein and not of the denaturant (*8*).

In the third class of proteins previously defined, GdnHCl is observed to alter nonlinearly the thermodynamic character of the N state ensemble (and possibly the thermodynamic character of the D ensemble) but with the effect on the N state ensemble occurring within the transition zone. That is, for this class, GdnHCl is inducing *variable thermodynamic character in the native ensemble within the transition zone*. These thermodynamic changes occurring "within" the native ensemble are taking place within the same concentration range that the denaturant is shifting the ratio between N and D. The dual thermodynamic effects taking place in the transition zone result in a $\Delta G^{\circ}_{N\rightarrow D}$ value from GdnHCl-induced denaturation that does not have the molecular level meaning commonly ascribed to it. Because the ratio between the native and denatured states is changing while the thermodynamic character of the native state itself is also changing, the transition represents no specific N ↔ D equilibrium in which the end states (N and D) are fixed or distinct; rather, it represents a constantly changing (variable) set of N ↔ D equilibria, with the native ensemble at the beginning of the transition being *thermodynamically different* from the native ensemble at the end of the transition (*8*).

Because spectroscopic observables are very useful in detecting the interconversion of N and D states, they enjoy widespread use in denaturation measurements. Although they are sensitive in detecting what may be defined as "between states" effects, which are the population shifts between N and D ensembles occurring in the denaturation transition zone, spectroscopic signals are not particularly sensitive to thermodynamic changes that denaturants can induce within the individual N or D ensembles, changes that we define as "within state" effects. Denaturation focuses on the shifts in populations of N and D states, so there has been a natural tendency to focus only on between states effects. This emphasis has left the subtle but nonetheless important within state effects relatively unrecognized or undetected. Because of the relative insensitivity of spectral observables to within state effects, it is necessary to detect and investigate such effects by alternative means. Through trial and error, we have found that thermodynamic observables and/or physical characterizations are much better suited for detecting and monitoring within state effects on the N and D ensembles. In particular, we note that Stokes radius measurements provide a sensitive way of characterizing the individual (N and D) ensembles and that determination of proton uptake/release of the ensembles as a function of denaturant concentration can also be an excellent way to monitor their thermodynamic characters.

Here, we undertake a comprehensive study of a protein that exhibits within state and between states effects of denaturants on the thermodynamics of denaturant-induced unfolding. The protein, which is referred to here as β1, is a mutant form of the protein G B1 domain. β1 has no disulfide bonds or prolyl residues and denatures in GdnHCl with a low $C_{1/2}$ value that is characteristic of proteins that exhibit "variable" thermodynamic character (*8*, *9*). Using urea and GdnHCl, our objective is to characterize β1 denaturation in terms of its denaturation thermodynamics, with emphasis on the evaluation and interpretation of between states and within state effects.

MATERIALS AND METHODS

Chemicals. Ultrapure GdnHCl was purchased from Amresco, high-purity urea was obtained from Nacalai, Tesque, Inc., sodium chloride was from Fisher, and sodium acetate was from Mallinckrodt. All other chemicals used were of either analytical or reagent grade. Concentrations of GdnHCl and urea solutions were determined from refractive index measurements at 25.0 ± 0.1 °C on a Milton Roy

refractometer with the temperature controlled by a water bath, using the relationships:

$$[\text{GdnHCl}] = 57.147\Delta n + 38.68\Delta n^2 - 91.6\Delta n^3 \quad (1)$$

$$[\text{urea}] = 117.66\Delta n + 29.753\Delta n^2 + 185.56\Delta n^3 \quad (2)$$

where Δn is the difference between the refractive index of the denaturant solution and the buffer solution (*2*).

Protein Expression and Purification. The plasmid construct for the T2Q, I6A, T44A protein G B1 domain (β1) was kindly provided for us by Prof. Lynne Regan. Details on the preparation of the construct were described previously (*9*). The construct was checked for the correct insert by sequencing (DNA Sequencing Laboratory, UTMB) and transformed into the *Escherichia coli* T7 expression strain BL21(DE3). Purification of β1 was performed on the basis of Regan's description with modifications described below (*9*). Transformed cells were grown in LB media at 37 °C with shaking until the OD_{600} reached about 0.6−0.7 (4−5 h) and then induced by adding IPTG (1 mM final concentration). Cells were grown for about an additional 2.5 h, harvested and collected by centrifugation, resuspended in pH 7 buffer (20 mM Tris-HCl, 1 mM EDTA), frozen at −80 °C, thawed, sonicated, and then centrifuged to remove cell debris. The crude lysate was mixed with poly(ethylenimine) (∼0.4% v/v) to precipitate contaminating nucleic acids and centrifuged to separate the precipitate. The supernatant was passed through a 0.45 μm filter and then mixed with Q-Sepharose (Pharmacia) beads (using about 100 mL of hydrated resin/5 L culture) preequilibrated in pH 7 buffer. After the pH was adjusted to 9, the mixture was incubated in ice with stirring overnight. The matrix was then packed in a glass column, washed with 1 column volume of buffer adjusted to pH 8, washed again with 3−4 column volumes of pH 7 buffer, and then eluted with pH 7 buffer containing 50 mM NaCl. Elutions were concentrated either by filter centrifugation or by putting the solution inside 3 kDa MW cutoff dialysis tubing and then covering the solution-filled dialysis bag with solid 20 kDa poly(ethylene glycol). The concentrated protein solution was purified further by size exclusion chromatography with a Sephadex G-50 (Sigma) column, using pH 7 buffer containing 50 mM NaCl. The purity of the final product was verified using SDS−PAGE and analytical size exclusion chromatography. The molecular weight was verified using matrix-assisted laser desorption/ionization time-of-flight (MALDI-TOF) mass spectrometry (Mass Spectrometry Facility, UTMB). Purified protein solutions were stored in 50 mM NaCl, 20 mM Tris-HCl, 1 mM EDTA, and 15% glycerol, pH 7 at −80 °C.

Protein concentrations were determined spectrophotometrically using the Edelhoch method (*10*−*12*). Extinction coefficients of 9530 and 5970 M^{-1} cm^{-1} were used for 280 and 288 nm, respectively. Protein concentrations determined at the two wavelengths were always in agreement (with less than 3% difference), suggesting the absence of spectrally detected impurities.

Protein Unfolding Measurements Using Spectroscopic Methods. Denaturation measurements were performed by mixing appropriate proportions of stock denaturant solution (e.g., 7.5 M GdnHCl, 0.2 M NaCl, 20 mM sodium acetate, pH 5.0), buffer solution (e.g., 0.2 M NaCl, 20 mM sodium acetate, pH 5.0), and protein solution (e.g., 1 mg/mL β1, dialyzed exhaustively against 0.2 M NaCl, 20 mM sodium acetate, pH 5.0), followed by incubation at 25 °C for 4−12 h and spectral determination. Unfolding measurements involving the use of urea were completed within 24 h after preparation of the urea solutions.

Fluorescence measurements were conducted using a SPEX FluoroMax spectrofluorometer. Fluorescence intensity (normalized to the lamp intensity) was monitored at excitation wavelengths of 275 and 295 nm, and emission at 340 nm, with excitation and emission bandwidths of 3−5 nm, depending on the protein concentration (about 5−10 μg/mL). Fluorescence recordings were made using a 1 cm path length cuvette, maintaining temperature at 25.0 ± 0.1 °C. Corrections were made for buffer and denaturant contributions to the fluorescence intensity.

CD measurements were carried out using an Olis RSM CD spectrometer. Ellipticity was monitored at 222 nm using a 0.1 cm path length cuvette thermostated at 25.0 ± 0.1 °C. Protein concentrations used ranged from 0.2 to 0.3 mg/mL. All measurements were corrected for buffer and denaturant CD contributions.

Absorbance spectra were recorded using a Model 14DS AVIV UV−vis spectrophotometer equipped with a Peltier automated temperature control unit, with all measurements conducted at 25.0 ± 0.1 °C, using protein concentrations ranging from 0.2 to 0.3 mg/mL. Spectra were recorded from 320 to 250 nm every 0.1 nm with 1 nm bandwidth and 1 s averaging time, using a pair of matched tandem 1 cm path length cuvettes. Savitzky−Golay filtering was performed twice on the spectral data using AVIV software to acquire second-derivative UV spectra (*13*). The first filtering involved using a 20-pt moving window size for third degree polynomial approximations, with zero-order derivatives taken. The second filtering involved using a 25-pt moving window for third degree polynomial approximations, and second-order derivatives were taken.

The degree of protein tyrosine exposure was calculated from the second-derivative spectra as described previously (*14*). The parameter, r_p, is defined as the ratio between two peak-to-peak distances (i.e., one between the maximum at ∼287 nm and the minimum at ∼283 nm and one between the maximum at ∼295 nm and the minimum at ∼290.5 nm), which, for a given protein tyrosine and tryptophan composition, is determined mainly by the polarity of the tyrosine environment. The degree of β1 tyrosine exposure (α) was calculated using the equation:

$$\alpha = (r_i - r_a)/(r_u - r_a) \quad (3)$$

where $r_i = [(\delta^2A/\delta\lambda^2)_{287} - (\delta^2A/\delta\lambda^2)_{283}]/[(\delta^2A/\delta\lambda^2)_{295} - (\delta^2A/\delta\lambda^2)_{290.5}]$; r_u is the r_p of the protein when completely unfolded; r_a is the r_p of a mixture containing the same molar ratio of aromatic amino acids as the protein and dissolved in a solvent possessing the same properties as the interior of the protein. Using ethylene glycol as a model for the protein interior, the following equation was used to estimate r_a (*14*):

$$r_a = (-0.18x + 0.64)/(-0.04x + 1) \quad (4)$$

where x is the ratio between the number of tyrosine and the number of tryptophan residues on the protein. On the basis

of the properties of model compounds in 6 M GdnHCl, r_u was estimated using the equation (*14*):

$$r_u = (0.20x + 0.66)/(-0.09x + 1) \quad (5)$$

Data from unfolding measurements (detecting spectral or nonspectral observables) were analyzed using the two-state linear extrapolation model and nonlinear least-squares fitting (*3*). All nonlinear least-squares analyses were performed using Origin (OriginLab) and/or Kaleidagraph (Synergy).

$\Delta\nu$ Measurement Apparatus. All $\Delta\nu$ measurements were carried out using a pHM85 Precision pH meter (Radiometer) equipped with a temperature probe and a calomel combination electrode (model GK473901, Radiometer), along with a Metrohm E415 pH-stat titration vessel. The titration vessel was thermostated at 25.0 ± 0.1 °C and was constantly flushed with purified nitrogen gas previously passed through three successive scrubbers: the first containing alkaline 1 M $BaCl_2$, the second containing 2 M phosphoric acid, and the third containing a solution identical in nonprotein composition with the solution being titrated. Titrants were delivered using MICROLAB dispensers (Hamilton) equipped with either a 250 or 1000 μL Hamilton syringe. Solutions being titrated were stirred at a constant rate with a Teflon-coated magnetic stirring bar.

Prior to titration measurements, pH meter readings were standardized using certified standard buffer solutions from Compliance Technology Inc. (pH 4.000 ± 0.002, pH 7.000 ± 0.002, pH 3.000 ± 0.002, and pH 10.000 ± 0.005). Two-point calibrations were performed using the pH 4 and 7 standard buffers. Linearity of pH meter readings outside the pH range of 4−7 was then tested using the pH 3 and 10 buffers, with deviations being less than 0.01 pH unit. No sodium ion error correction was necessary until pH >10. The manufacturer of the calomel electrode used recommends correction at pH >12.

HCl Titrant Concentration Determination. Concentrations of HCl titrants were calibrated using ultrapure Tris base (ICN) as the primary standard. Tris solution was volumetrically prepared by dissolving preweighed Tris base (oven-dried at 60 °C overnight) and NaCl (0.2 M) in freshly degassed Milli-Q water (18.2 MΩ-cm). A 5.00 mL volume (V_{Tris}) of Tris solution was delivered into the titration vessel and flushed with nitrogen for 5 min. The Tris solution was titrated using fixed volume aliquots of 3 μL of HCl titrant (0.2 M NaCl) with a 15 s time interval between each aliquot, recording the total volume of HCl titrant added (V_{HCl}) and the corresponding pH. The equivalence point was determined using two forms of Gran's graphical method (*15*). The first method involves a plot of Φ against V_{HCl}, where Φ is defined as

$$\Phi \equiv (V_{Tris} + V_{HCl}) \times 10^{-pH} \quad (6)$$

Below the equivalence point (V_e), Φ is approximately constant, but beyond V_e, Φ varies linearly with V_{HCl} and is expressed as

$$\Phi = -a + b(V_{HCl}) \quad (7)$$

V_e is then determined as the value of V_{HCl} at $\Phi = 0$ (i.e., a/b). Knowing the concentration of Tris in the initial Tris solution ([Tris]), the concentration of HCl in the titrant (M_{HCl}) can then be calculated as

$$M_{HCl} = [Tris](V_{Tris})/V_e \quad (8)$$

The second method involves plotting Ψ vs V_{HCl}, where Ψ is defined as

$$\Psi \equiv V_{HCl} \times 10^{pH} \quad (9)$$

As V_{HCl} approaches V_e from the preequivalence point region, Ψ varies linearly with V_{HCl}, and Ψ may be expressed as

$$\Psi = -c + d(V_{HCl}) \quad (10)$$

V_e is the value of V_{HCl} at $\Psi = 0$ (i.e., c/d). M_{HCl} is then calculated in the manner as that described above (eq 8).

HCl titrant concentration calibrations were performed multiple times, employing the two forms of Gran plots each time for better determination of titrant concentrations. Since the two methods described make use of different regions of the titration data, agreement between the methods serve to validate calibration results. Deviations between the two methods are always less than 2% of the calculated titrant concentration. Least-squares analyses of the Gran plots, as described by eqs 7 and 10, were performed using either Origin or Kaleidagraph.

$\Delta\nu$ Measurements. Changes in the number of moles of protons bound per mole of protein ($\Delta\nu$) with increasing GdnHCl concentrations were monitored in 0.2 M NaCl, pH 3.500, at 25.0 ± 0.1 °C, taking 0 M GdnHCl as the reference. Protein samples (3−5 mg/mL) were dialyzed against deionized distilled water (18.2 MΩ-cm) multiple times at 0−4 °C, pH ~3.6. Solutions of 7.5 M GdnHCl, 0.25 M NaCl, pH ~7.1, and 0.25 M NaCl, pH ~3.7, were prepared using freshly degassed 18.2 MΩ-cm water. The previously dialyzed protein solution (1.00 mL) was dispensed into the titration vessel. After thermal equilibration of the protein solution, $\{4000 - ([GdnHCl]_i/7.5) \times 5000\}$ μL of 0.25 M NaCl solution was added, where $[GdnHCl]_i$ is the target final GdnHCl molar concentration. The protein−NaCl solution was allowed to equilibrate to 25.0 °C, adjusted to exactly pH 3.500, and then mixed with $\{([GdnHCl]_i/7.5) \times 5000\}$ μL of 7.5 M GdnHCl and 0.25 M NaCl solution. The final protein−NaCl−GdnHCl solution was allowed to equilibrate at 25.0 °C for at least 5 min and then was titrated back to pH 3.500. The volume of HCl titrant added $\{V_{HCl}(protein)\}$ was recorded. In general, at acidic pH, protein unfolding results in proton uptake. To account for nonprotein contributions in the proton uptake process, the same titration experiment as described above was conducted on the dialysate. The volume of HCl titrant $\{V_{HCl}(blank)\}$ needed to titrate back to exactly pH 3.500 was also recorded. $[GdnHCl]_i$ was chosen to span a range from 0 to 4 M GdnHCl, and enough data were obtained to describe the protein N to D transition. Knowing the total number of moles of protein present in the experiment, $\Delta\nu$ was then calculated using the equation

$$\Delta\nu = (\{V_{HCl}(protein) - V_{HCl}(blank)\}M_{HCl})/(\text{mole of protein}) \quad (11)$$

where M_{HCl} is the molar concentration of the titrant.

Size Exclusion Chromatography. Size exclusion chromatography (SEC) measurements were conducted using a Phenomenex BioSep SEC-S2000 300 × 7.80 mm steel-jacketed HPLC gel filtration column and a fully automated BioCad SPRINT HPLC system. The column temperature was maintained at 25.0 ± 0.1 °C using an HPLC column water jacket supported by a circulating water bath. Protein solutions (0.4 mg/mL β1) were incubated in the appropriate solution (0.2 M NaCl, 20 mM sodium acetate, 0−8.5 M urea, pH 5.0) for at least 1 h before injection (using a 50 μL sample volume) into the column previously equilibrated in the same solution. All runs were carried out at a flow rate of 1 mL/min and were reproducible to within ±0.01 mL elution volume. For more accurate characterization of the protein system, blue dextran and sodium azide were also applied to the column under the same condition as the protein samples. This permitted calculation of the partition coefficient (K_d) at each urea concentration, as shown in the equation:

$$K_d = (V_e^{\text{protein}} - V_e^{\text{blue dextran}})/(V_e^{\text{azide}} - V_e^{\text{blue dextran}}) \quad (12)$$

where V_e^{protein}, $V_e^{\text{blue dextran}}$, and V_e^{azide} represent the elution volumes of β1, blue dextran, and sodium azide, respectively.

Prior to the experimental measurements, column calibration was performed to determine the functional relationship between the reciprocal of the partition coefficients ($1/K_d$) and protein Stokes radii, using proteins of known Stokes radius either in native conditions or in the presence of 8 M urea, as reported in the literature and as compiled by Uversky (*16*) and Corbett and Roche (*17*). As models for folded proteins, BSA, chymotrypsinogen A, cytochrome *c*, β-lactoglobulin, myoglobin, and ribonuclease A were chromatographed in 30 mM MOPS, 0.1 M NaCl, and 2 mM EDTA, pH 7.0. Likewise, to represent urea-unfolded proteins, SEC of chymotrypsinogen A, insulin, β-lactoglobulin, and ribonuclease A was carried out in 8 M urea, 20 mM DTT, 30 mM MOPS, 0.1 M NaCl, and 2 mM EDTA, pH 7.0. With the column used in this study, $1/K_d$ relates to the Stokes radius in a curvilinear fashion, with increasing column sensitivity to dimensional changes as the protein Stokes radius becomes larger. In the protein size range for the urea-induced unfolding of β1, $1/K_d$ versus Stokes radius is linear. Importantly, SEC data for both the folded and urea-unfolded proteins can be described by a single calibration curve, which suggests that changes in $1/K_d$ with increasing urea concentrations can be safely assumed to reflect changes in protein dimensions and not in the column matrix properties.

Dynamic Light Scattering. Dynamic light scattering (DLS) measurements were conducted at 25.0 ± 0.2 °C. Prior to measurements, protein solutions (1.5−2.5 mg/mL β1) were incubated at the appropriate solution conditions (0.2 M NaCl, 20 mM sodium acetate, pH 5.0, and 0−2 M GdnHCl or 0−8 M urea) for at least 30 min and then filtered through 0.02 μm Anodisc filters (Whatman). Duplicates of protein samples at each denaturant concentration were prepared. DLS measurements were performed using a DynaPro-MS/X dynamic light scattering instrument (Protein Solutions, Inc.) equipped with a 248-channel autocorrelator with multi-tau scheme starting at 0.48 μs delay time and an automated temperature control unit. A semiconductor laser of 822.6 nm provides the light source, with the scattered light collected at an angle of 90° and guided via a fiber optic cable to an actively quenched, solid-state single photon counting module, where light is converted to electrical signal. Fluctuations in the scattered light intensity as a function of time are analyzed by autocorrelation. Autocorrelation functions were generated every 5 s, collecting data for at least 3 min per sample. Data analysis was performed using the program Dynamics (Protein Solutions, Inc.). Single-exponential autocorrelation function baselines that are not within 1.000 ± 0.001 were discarded. Remaining autocorrelation functions were then analyzed using the intensity-weighted regularization model provided in the Dynamics software. The output of the analysis is the translational diffusion coefficient (D_T) of the particles in solution, which is then automatically converted to the Stokes radius (R_S) of the particles, assuming Brownian motion and the Stokes−Einstein equation:

$$R_S = (k_b T)/(6\pi\eta D_T) \quad (13)$$

where k_b is the Boltzmann constant, T is the temperature in kelvin, and η is the solvent viscosity. Solvent refractive indices and viscosities (which are needed in the determination of D_T) were provided as inputs for the software. Solvent refractive indices were measured with a refractometer and/or estimated by employing eq 1 for the GdnHCl solutions or eq 2 for the urea solutions, solving numerically for Δn, and calculating the refractive index for the denaturant solutions from Δn and the measured refractive index of the buffer in the absence of denaturants. Refractive index estimations resulted in deviations that do not exceed 0.2% of the value, in cases where both measurement and estimation were performed. Solvent viscosities in the presence of GdnHCl and urea, on the other hand, were estimated following the suggestion of Kawahara and Tanford (*18*). On the basis of their viscosity data, the following relationships on the molar concentration dependence of the viscosities of aqueous solutions of GdnHCl (η_{Gdn}) and urea (η_{urea}) at 25 °C were acquired:

$$\eta_{Gdn} = 0.8904 + 0.02132M_{Gdn} + 0.01359(M_{Gdn})^2 - 0.00219(M_{Gdn})^3 + 0.00032(M_{Gdn})^4 \quad (14)$$

$$\eta_{urea} = 0.8828 + 0.03321M_{urea} + 0.00275(M_{urea})^2 + 0.00028(M_{urea})^3 \quad (15)$$

where viscosities are expressed in centipoise, M_{Gdn} is the molar concentration of GdnHCl, and M_{urea} is the molar concentration of urea (for eqs 14 and 15, $R^2 = 0.99996$ and 1, respectively). To correct for the viscosity contributions of other solution components, mainly just 0.2 M NaCl (ignoring contributions from the 20 mM sodium acetate buffer), the concentration of GdnHCl (0.53 M) or urea (0.46 M) which alone would give the same viscosity as the 0.2 M NaCl aqueous solution was determined on the basis of literature data on the viscosities of NaCl solutions at 25 °C (*19*). GdnHCl or urea solutions were considered to have effective concentrations equal to the actual concentrations plus 0.53 M (for GdnHCl) or 0.46 M (for urea). The calculated effective concentrations were then used as inputs for eqs 14 and 15 to calculate solution viscosities.

Differential Scanning Calorimetry. The thermal unfolding behavior of β1 in the presence of varying concentrations of

Table 1: Thermodynamic Parameters for the GdnHCl- and Urea-Induced Unfolding of $\beta 1$[a]

observable	$\Delta G^{\circ}_{N\rightarrow D}$ (kcal/mol)	*m*-value (kcal mol^{-1} M^{-1})	$C_{1/2}$ (M)
GdnHCl Denaturation Parameters			
fluorescence (λ_{ex} = 275 nm; λ_{em} = 340 nm)	2.76 ± 0.13[b]	−2.20 ± 0.09[b]	1.26 ± 0.03[b]
fluorescence (λ_{ex} = 295 nm; λ_{em} = 340 nm)	2.74 ± 0.18[b]	−2.18 ± 0.03[b]	1.26 ± 0.04[b]
far-UV CD (222 nm)[e]	2.31 ± 0.13	−1.95 ± 0.07	1.18 ± 0.07[d]
far-UV CD (222 nm)[f]	2.77 ± 0.07	−2.21 ± 0.06	1.25 ± 0.04[d]
second-derivative UV[g]	2.53 ± 0.39	−2.00 ± 0.22	1.27 ± 0.19[d]
tyrosine exposure	2.79 ± 0.61	−2.27 ± 0.38	1.23 ± 0.28[d]
Urea Denaturation Parameters			
fluorescence (λ_{ex} = 275 nm; λ_{em} = 340 nm)	3.92 ± 0.54[c]	−0.87 ± 0.08[c]	4.48 ± 0.21[c]
fluorescence (λ_{ex} = 295 nm; λ_{em} = 340 nm)	3.88 ± 0.36[c]	−0.86 ± 0.06[c]	4.50 ± 0.15[c]
far-UV CD (222 nm)	3.76 ± 0.12[c]	−0.85 ± 0.01[c]	4.44 ± 0.06[c]
second-derivative UV[g]	3.74 ± 0.31	−0.85 ± 0.07	4.42 ± 0.12[d]
tyrosine exposure	3.02 ± 0.61	−0.67 ± 0.13	4.51 ± 0.28[d]
$1/K_d$ (size exclusion chromatography)	3.62 ± 0.29	−0.81 ± 0.06	4.47 ± 0.12[d]
Stokes radius (dynamic light scattering)	3.47 ± 0.63	−0.79 ± 0.15	4.39 ± 0.26[d]

[a] Unless stated otherwise, errors reported are fitting errors. [b] Errors reported are the standard deviation of four measurements. [c] Errors reported are the standard deviation of triplicate measurements. [d] Errors estimated by propagating the reported error for $\Delta G^{\circ}_{N\rightarrow D}$ and the *m*-value. [e] Predenaturation baseline defined by the nonlinear least-squares fitting program (larger slope in Figure 1B). [f] Predenaturation baseline defined by the operator (smaller slope shown in Figure 1B). [g] Errors reported are the average of fitting errors derived from the independent nonlinear least-squares analysis of unfolding data at different wavelengths.

NaCl was investigated via differential scanning calorimetry using a Microcal VP-DSC instrument. Scanning from 25 to 100 °C, a scan rate of 1 deg min^{-1} was employed in the experiments, which is enough for the protein system to reach equilibrium since a scan rate of 0.5 deg min^{-1} gave virtually the same results, within error limits. Rescans of previously scanned samples showed $\beta 1$ thermal denaturation to be reversible, even when the initial scans were carried out to ~100% completion (i.e., with >90% recovery of the signal). Protein concentrations ranged from 0.22 to 0.24 mM. Calorimetric profiles were analyzed using the Microcal Origin software (Microcal Software, Inc.), employing a two-state model.

RESULTS

In evaluating the equilibrium thermodynamics of protein denaturation, it is essential to first establish whether the denaturation is two-state and reversible. One of the principal tests of two-state behavior involves demonstration that the same ratio of N and D species is obtained as a function of denaturant concentration regardless of which observable is used to monitor the N → D transition. Two-state denaturation requires the transition to be all or none; i.e., at equilibrium the protein is comprised of two populations (N and/or D states) with no substantive populations of partially folded states. Monitoring various protein properties that report on different parts of the protein can be helpful in determining whether all parts of the protein denature coordinately as required of the two-state hypothesis. To observe tertiary structural characteristics, we used fluorescence spectroscopy to monitor changes in the fluorescence properties of the single tryptophan residue of $\beta 1$ by itself (with the excitation wavelength set at 295 nm) and in coordination with the fluorescence properties of the three tyrosine residues of $\beta 1$ (excitation wavelength set at 275 nm). Changes in the secondary structure of $\beta 1$ were detected by means of far-UV CD spectroscopy, monitoring ellipticity at 222 nm. In addition, second-derivative UV spectroscopy was used to detect changes in the polarity of the tyrosine environments upon denaturation.

Figure 1 presents a summary of data obtained using the mentioned spectral observables to monitor the GdnHCl-induced unfolding of $\beta 1$. Specifically, Figure 1A provides representative fluorescence data (275 nm excitation, 340 nm emission), Figure 1B presents data on far-UV CD, and panels C−E of Figure 1 show data on second-derivative UV spectroscopy. Figure 1F presents a summary of the GdnHCl unfolding data, showing the degree of coincidence of the fractional ratio (D/N) as monitored by the various spectral observables. The reversibility of $\beta 1$ GdnHCl-induced unfolding was assessed by including reversibility points for a number of the GdnHCl denaturation measurements performed (as shown, for example, in Figure 1B,E). The reversibility points, obtained by refolding denatured $\beta 1$, are observed to coincide with unfolding data obtained for the GdnHCl-induced unfolding of $\beta 1$. Thermodynamic evaluations of the data in Figure 1A−E are provided in Table 1. In all cases except CD-monitored GdnHCl-induced denaturation the results show overlap in $\Delta G^{\circ}_{N\rightarrow D}$ values.

Dynamic light scattering (DLS) was used to monitor the Stokes radius of the protein as a function of GdnHCl concentration. The protein Stokes radius, as presented in Figure 2, provides physical characterization of the N and/or D ensembles in GdnHCl and in urea, respectively. The DLS data for GdnHCl unfolding was not analyzed using the LEM due to nonlinear behavior in the predenaturation baseline and because, above 2 M GdnHCl, denatured $\beta 1$ gives erratic DLS results, presumably because of denatured protein−protein association at the high protein concentrations (1.5−2.5 mg/mL) needed in these experiments. Thus, we were only able to track the Stokes radius of $\beta 1$ to slightly above 2 M GdnHCl. At low GdnHCl concentrations (0−1 M), the Stokes radius data for $\beta 1$ appear to be hyperbolic from 0 to 0.5 M GdnHCl, before beginning to take on the usual sigmoid dependence expected in protein unfolding. For comparison, the fraction of unfolded $\beta 1$ as calculated from the fluorescence data of Table 1 is superimposed on the Stokes radius data in Figure 2A. The deviation of the Stokes radius data between 0 and 0.5 M GdnHCl indicates a measurable expansion of the N state ensemble, occurring within the first 10% of the unfolding transition. With the

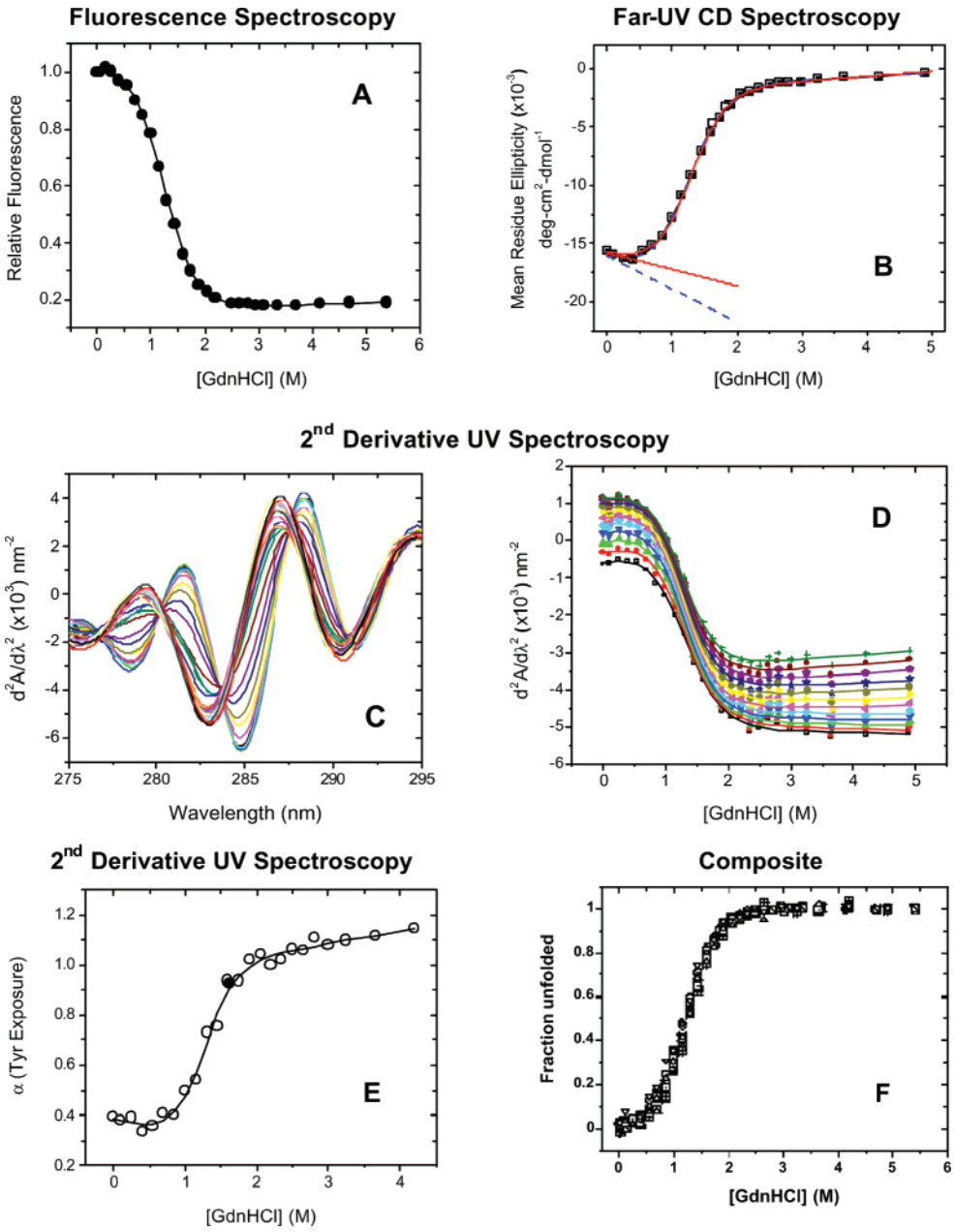

FIGURE 1: β1 GdnHCl-induced denaturation monitored by different spectroscopic techniques. GdnHCl-induced unfolding measurements were performed in 0.2 M NaCl and 20 mM sodium acetate, pH 5.0 at 25.0 °C, using fluorescence, far-UV CD, and second-derivative UV spectroscopy. Tryptophan and/or tyrosine fluorescence was monitored as a function of GdnHCl concentration using excitation wavelengths of 275 and 295 nm, respectively, and an emission wavelength of 340 nm. Four separate fluorescence experiments were carried out four times, giving the representative data in (A). Shown in (B) are 222 nm CD data on β1 GdnHCl-induced unfolding. Two linear predenaturation baselines are shown: (1) the solid baseline is operator-defined and is a linear least-squares fit of all points in the predenaturation concentration range, and (2) the dashed line was defined by a nonlinear least-squares fit of all of the CD data to the LEM. (C) gives β1 second-derivative UV spectra at different GdnHCl concentrations, with β1 samples at higher GdnHCl concentrations exhibiting blue-shifted spectra relative to that of samples at lower concentrations. Four regions of the second-derivative spectra were analyzed as slices of constant wavelength and varying GdnHCl concentrations, i.e., 281.5−282.6, 284.6−285.5, 285.5−287, and 288.1−290 nm. The data shown in (D) represent the slices in the 281.5−282.6 nm region. Unfolding data at each wavelength were analyzed indepenedently using the LEM. In (E) are results representing the dependence of the solvent accessibility of β1 tyrosine residues on GdnHCl concentration, calculated from the second-derivative spectra as discussed in the Materials and Methods section. Sigmoid curves shown in (A), (B), (D), and (E) are the LEM nonlinear least-squares best fits of the respective data, assuming linear baselines. [The sigmoid curves in (B) represent fitting results where the predenaturation baseline slope parameter is either floated (blue) or defined so that the predenaturation baseline coincides with the 0−0.4 M GdnHCl data points; the straight lines are the corresponding predenaturation baselines, using the same color scheme.] (F) represents a summary of the described GdnHCl unfolding measurements, showing all of the fluorescence and far-UV CD spectroscopy data and representatives for each analyzed spectral region in the second-derivative UV spectroscopy data, plotting the fraction of unfolded protein as a function of GdnHCl concentration. Also shown in (B) and (E) are reversibility points. (For details on the protein concentrations used, refer to Materials and Methods.)

possible exception of the CD measurements in Figure 1B, data from the other spectral observables provide little or no corroborative evidence of effects in the predenaturation zone.

The population-weighted Stokes radius of the protein as a function of urea concentration (Figure 2B) differs significantly from that in GdnHCl. Prior to onset of the urea-

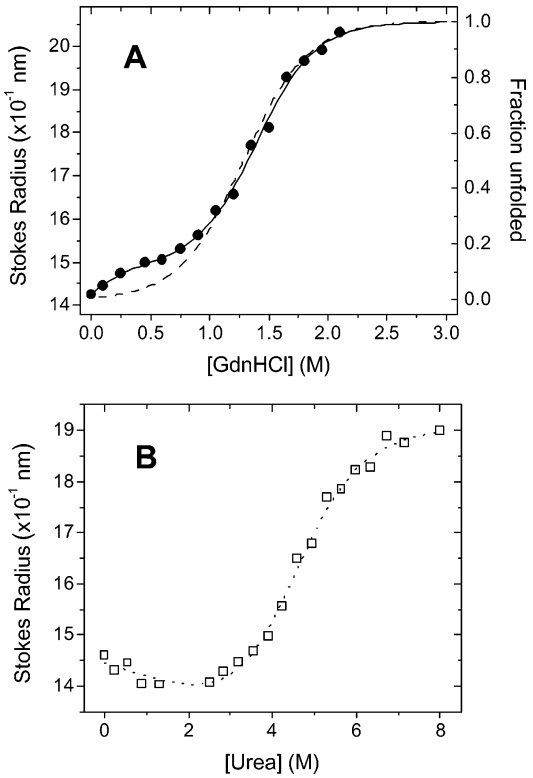

FIGURE 2: β1 GdnHCl-induced (and urea-induced) unfolding monitored by dynamic light scattering. Panel A: GdnHCl unfolding measurements were performed in 0.2 M NaCl and 20 mM sodium acetate, pH 5.0 at 25.0 °C, detecting changes in protein dimension as a function of GdnHCl concentration (●). The dashed curve represents the fraction of folded protein determined using fluorescence data shown in Figure 1A. Panel B: β1 urea denaturation was also performed under the same experimental conditions as listed above (□). The dashed curve is the LEM nonlinear least-squares best fit curve of the urea-induced unfolding data.

induced denaturation transition, there appears to be a small decrease in the Stokes radius of β1 over the 0−2 M urea concentration range. Given the noise of the data within this range, the decrease in Stokes radius may only be apparent, so the result was later investigated using size exclusion chromatography data (see below), which is of higher quality. Using the LEM, we were able to fit the urea data shown in Figure 2B, and the results of the fit are presented in Table 1. It is important to note that, at 2 M GdnHCl, the Stokes radius of the GdnHCl D ensemble of β1 is measurably larger than the D ensemble in 8 M urea. The equivalent volume for the GdnHCl D ensemble as defined by the Stokes radius in 2 M GdnHCl is on the order of 35% larger than that of the D ensemble in 8 M urea.

Difficulty in finding observables to detect "within states" effects on N and D ensembles led us in previous work to use proton uptake/release as an observable (*7*, *8*, *20*, *21*). At the pH of interest, if the pK_as of one or more titrateable groups in the N state change when converted to the D state, a net proton uptake or release ($\Delta\nu$) will be observed. In fact, the quantity $\Delta\nu$ is a thermodynamic parameter capable of monitoring within state and between states thermodynamic changes occurring outside of and inside the transition zone (*8*). Unfortunately, in β1 the pK_as of carboxylic groups at pH 5 do not change on shifting N to D; thus $\Delta\nu$ is zero for the protein at this pH. To illustrate the point that within state and between states thermodynamic changes can occur

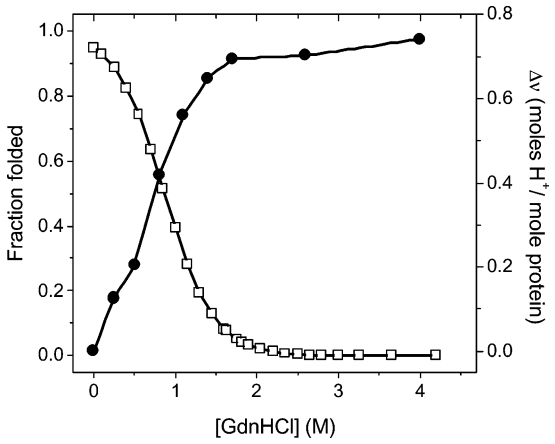

FIGURE 3: Proton uptake by β1 upon GdnHCl-induced unfolding monitored by potentiometry. $\Delta\nu$ measurements were performed as a function of GdnHCl concentration in 0.2 M NaCl at 25.0 °C, using pH 3.500 as the reference pH. Shown as a function of GdnHCl concentration is the degree of proton uptake, $\Delta\nu$ (●), compared to the fraction of folded protein (□), calculated using LEM-derived baseline parameters from GdnHCl unfolding data monitored via fluorescence spectroscopy in 0.2 M NaCl, 10 mM sodium acetate, 10 mM sodium phosphate, and 10 mM glycine, pH 3.50 at 25.0 °C. For the fluorescence data, $\Delta G^\circ_{N\rightarrow D}$ and the *m*-value were evaluated to be 1.70 ± 0.04 kcal/mol and −1.96 ± 0.01 kcal mol^{-1} M^{-1}, respectively.

simultaneously, we performed $\Delta\nu$ experiments at pH 3.5. At this pH, pK_as are shifted, and the results of these $\Delta\nu$ measurements are given in Figure 3. A plot of fractional folding of β1 determined from fluorescence measurements is provided in Figure 3 as a guide. It is evident from Figure 3 that significant $\Delta\nu$ changes occur within the transition zone (between states effects). There is also evidence of a $\Delta\nu$ of small magnitude occurring with the N ensemble (within states effects) in the range of 0−0.5 M GdnHCl. The same pattern of within state and between states effects of $\Delta\nu$ versus GdnHCl concentration has been observed with staphylococcal nuclease, but more data points were possible to obtain with this protein (*8*).

Returning to pH 5, Figure 1B suggests small apparent GdnHCl-induced changes in β1 ellipticity observed at predenaturation concentrations. The N state β1 ellipticity changes in the presence of GdnHCl are admittedly small. However, they are significant enough to cause the GdnHCl-induced LEM fit to give a $\Delta G^\circ_{N\rightarrow D}$ that is distinguishably smaller than the $\Delta G^\circ_{N\rightarrow D}$ values obtained using all other spectral observables (see Table 1). One reason for the variation in $\Delta G^\circ_{N\rightarrow D}$ values using GdnHCl is that the predenaturation range is short, and it was left to the nonlinear least-squares fitting program to define the predenaturation baseline. The predenaturation baseline of steepest slope in Figure 1B was obtained by allowing the slope and intercept to float in the fit of the data to the LEM. If an operator-defined baseline of smaller slope (solid straight line) is used as shown in Figure 1B, the resulting $\Delta G^\circ_{N\rightarrow D}$ and *m*-value parameters are well in line with results obtained using other spectral observables (see Table 1).

To assess whether fitting errors can be reliable estimates of experimental errors (and to check the reproducibility of our results), GdnHCl and urea denaturation measurements were performed on multiple samples, monitoring far-UV CD and/or tryptophan and tyrosine fluorescence. With the

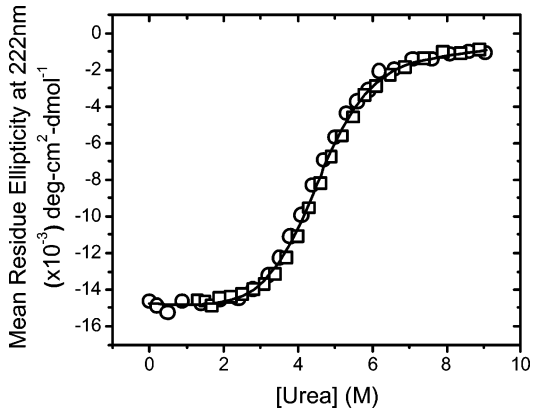

FIGURE 4: Urea-induced β1 denaturation monitored by far-UV CD spectroscopy. β1 unfolding measurements were performed in 0.2 M NaCl and 20 mM sodium acetate, pH 5.0 at 25.0 °C, employing fluorescence, far-UV CD, and second-derivative UV spectroscopy. Shown are data from urea unfolding (○) and refolding experiments (□) detected using far-UV CD spectroscopy. The curve represents the nonlinear least-squares best fit of the composite data to the two-state linear extrapolation model.

denaturation measurements on multiple samples, the errors obtained were not found to be significantly different from fitting errors obtained on analysis of single denaturation profiles. In general, experimental errors in our urea-unfolding measurements are larger than those in the GdnHCl denaturation measurements (see Table 1). The larger errors may be due to the longer extrapolation involved in using LEM in the case of urea, a generally less potent denaturant compared to GdnHCl (*2*). In addition, errors on the estimated thermodynamic parameters using tyrosine exposure from the second-derivative UV spectroscopy data are significantly larger than that of the other data. This is to be expected because the determination of tyrosine exposure (as described in the Materials and Methods section) involves more sources of error.

Whereas 222 nm ellipticity is sharply dependent on GdnHCl in the predenaturation concentration range (Figure 1B), no dependence of 222 nm ellipticity is observed with urea as the denaturant (see Figure 4). GdnHCl appears to cause changes in the Stokes radius and CD in the predenaturation concentration range suggestive of physical and perhaps structural and thermodynamic alterations in β1. By contrast, predenaturational concentrations of urea show no CD changes and little or no changes in the Stokes radius as determined by DLS. The appearance that GdnHCl causes changes in β1 at predenaturational concentrations while urea does not was investigated further.

Because of the noise in the DLS Stokes radius measurements using urea (Figure 2) and questions raised by the apparent decrease in the Stokes radius of the N ensemble in 0−2 M urea, size exclusion chromatography was used to corroborate the effects of urea on the dimensions of the N and D ensembles of β1. We have shown previously that the reciprocal of the size exclusion partition coefficient ($1/K_d$) is proportional to the Stokes radius of proteins (*22*). Figure 5A gives a plot of $1/K_d$ for β1 as a function of urea concentration, and the data were fitted to the LEM with the results reported in Table 1. In contrast to the DLS data of Figure 2, the more precise data on the dimensions of the β1 N and D ensembles reveal no change in the N state ensemble dimensions over the 0−1.5 M [urea] range. Thus, we

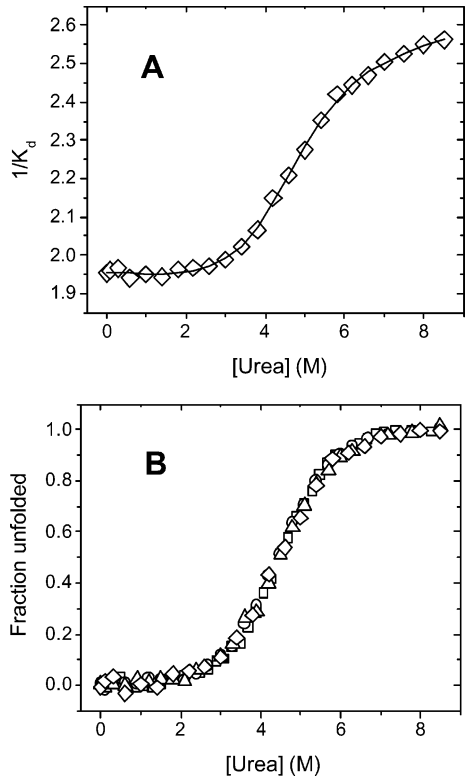

FIGURE 5: β1 urea-induced unfolding monitored via size exclusion chromatography. Measurements were performed in 0.2 M NaCl and 20 mM sodium acetate, pH 5.0 at 25.0 °C. The reciprocal of partition coefficient, $1/K_d$, is plotted against urea concentration in (A). Results of nonlinear least-squares fitting of the data to the LEM are given in Table 1. Shown in (B) is the summary of urea denaturation data, plotting the fraction of unfolded protein as a function of urea concentration, using representative fluorescence (□), far-UV CD (○) and second-derivative UV spectroscopy (△), and size exclusion chromatography (◇) data.

conclude that urea does not alter the dimensions of the N state ensemble. For sake of comparison, Figure 5B shows a composite plot of the β1 fraction unfolded extracted from urea-induced LEM data obtained using multiple observables. The results of LEM fits using fluorescence, CD, second-derivative spectroscopy, tyrosine exposure, size exclusion chromatography, and dynamic light scattering as observables are provided in Table 1. As indicated by Figure 5B and Table 1, within the error of the measurements, the multiple observables all give the same value of $\Delta G^\circ_{N\rightarrow D}$ for the urea-induced denaturation of β1.

As mentioned in the introduction, a key aspect of the interpretation of $\Delta G^\circ_{N\rightarrow D}$ depends on whether it is independent of the nature of the denaturant. When GdnHCl- and urea-induced denaturation results in $\Delta G^\circ_{N\rightarrow D}$ values that are not identical, it means that either one or both $\Delta G^\circ_{N\rightarrow D}$ values contain a denaturant-dependent free energy contribution. Figure 6A1−C1 give representative spectral data on the denaturation of β1 by urea and GdnHCl, and Figure 6A2−C2 show the results of LEM fits to these data. Clearly, GdnHCl-induced denaturation of β1 extrapolates to a $\Delta G^\circ_{N\rightarrow D}$ value that is about 1−1.2 kcal/mol less than that obtained from urea-induced denaturation. We are then left with determining which, if either, of the $\Delta G^\circ_{N\rightarrow D}$ values is independent of the nature of the denaturant.

Because GdnHCl is both a denaturant and a strong salt, in explaining the $\Delta G^\circ_{N\rightarrow D}$ discrepancy obtained with urea

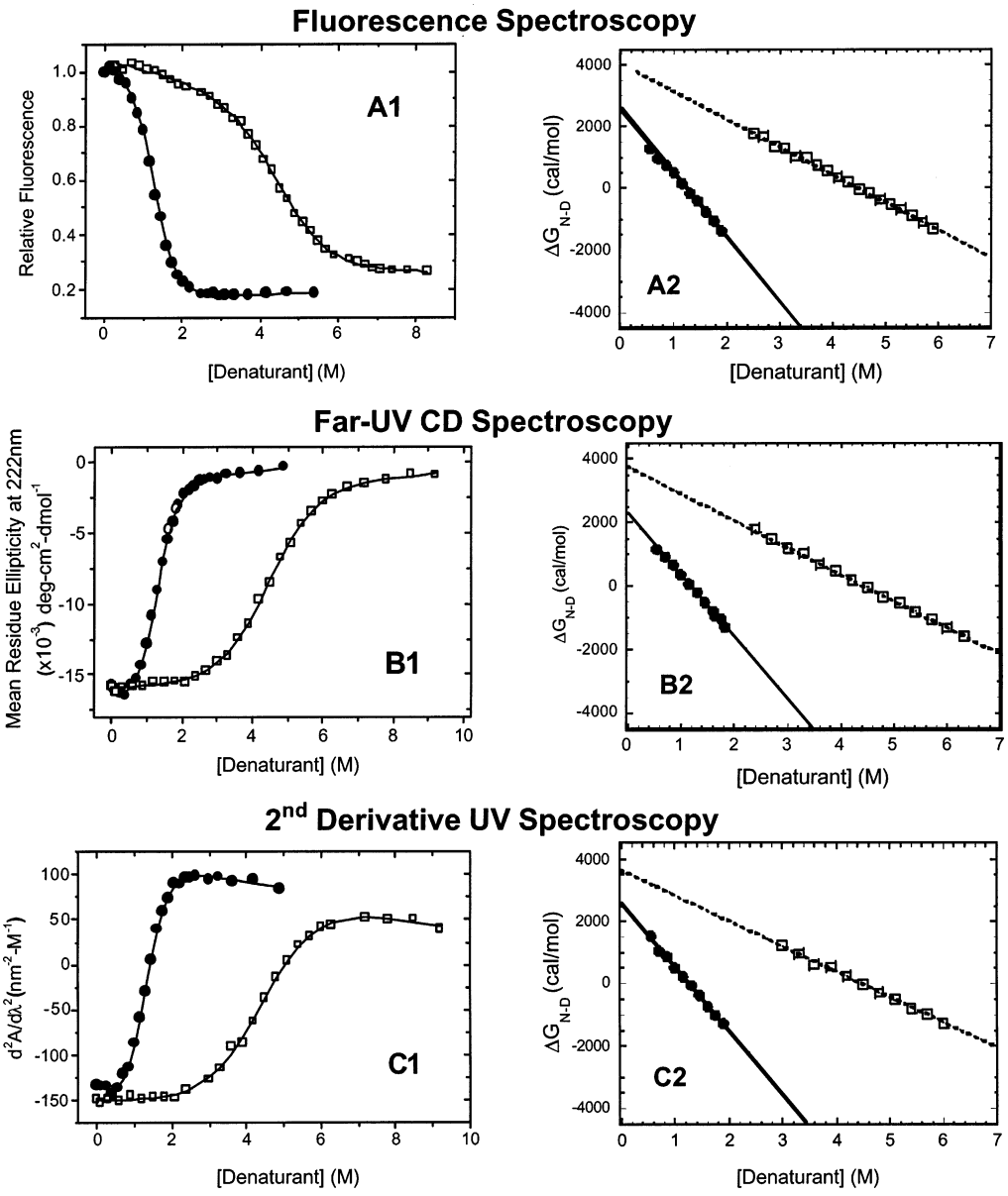

FIGURE 6: Comparison of the GdnHCl and urea denaturation profiles of β1. Shown in (A1), (B1), and (C1) are representative GdnHCl and urea unfolding data monitored by fluorescence, far-UV CD, and second-derivative UV spectroscopy (λ = 286 nm), respectively. Representations of the results of LEM analysis of the fluorescence, far-UV CD, and second-derivative UV spectroscopy data are shown in (A2), (B2), and (C2), respectively, plotting $\Delta G_{N\rightarrow D}$ as a function of denaturant concentration. GdnHCl unfolding data are represented by (●), while urea denaturation data are represented by (□).

and GdnHCl, an obvious possibility is that a salt effect may be decreasing the stability of the N state ensemble and that the $\Delta G^{\circ}_{N\rightarrow D}$ differences between urea- and GdnHCl-induced denaturation may arise from a salt effect on the N ensemble. Figure 7 provides some indication that NaCl, a neutral salt that is not generally considered to be a denaturant, has strong effects on the thermal stability of β1. Between 0.2 and 0.8 M NaCl, the temperature of the midpoint of thermal denaturation (T_m) is seen to decrease to a minimum at about 0.8 M NaCl, and β1 becomes stabilized by >0.8 M NaCl. We take this as suggestive evidence that salts can decrease β1 stability in the range from 0.2 to 0.8 M.

DISCUSSION

β1 denaturation induced by urea at pH 5 is much less complicated than that of its GdnHCl-induced denaturation. The pre- and postdenaturation baselines for urea-induced denaturation are all linear over a significant urea concentration range (Figures 2 and 4−6), making it rather easy for nonlinear least-squares analysis to give $\Delta G^{\circ}_{N\rightarrow D}$ values unbiased by the investigator. The results in Table 1 and Figure 5B demonstrate clearly that, regardless of the observable used in monitoring denaturation, the derived thermodynamic parameters and the unfolding data are fully consistent with the conclusion that urea-induced β1 denaturation is two-state and reversible. The same conclusion is drawn for GdnHCl-induced β1 denaturation at pH 5, but the Stokes radius results (Figure 2A) show important changes in the N state ensemble at GdnHCl concentrations preceding the onset of denaturation.

The multiple observable test for two-state denaturation seeks evidence that states of the protein which are not part of the N or D ensembles are populated under equilibrium conditions. As employed here, the rationale behind the test

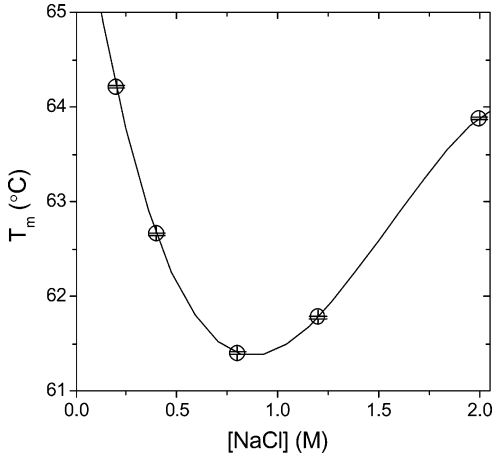

FIGURE 7: β1 thermal denaturation as a function of NaCl concentration monitored via differential scanning calorimetry. Plotted are thermal transition midpoints (T_m) versus salt concentration. Values for T_m were determined from DSC measurements performed in 20 mM sodium acetate, pH 5.0 at 25.0 °C, and 0.2, 0.4, 0.8, 1.2, or 2 M NaCl. The curve is drawn to show the trend.

is that, as a function of denaturant concentration, the chances of detecting the existence of additional equilibrium states should be enhanced through the use of multiple observables. Because it is unreasonable to be exhaustive in the number of observables used to monitor denaturation, in practice, the multiple observable test is incapable of delivering definitive proof in favor of the two-state hypothesis. Despite this flaw, it remains the most readily accessible test of denaturant-induced two-state behavior, and we use it here in comparing the thermodynamics of urea- and GdnHCl-induced denaturation of β1. Spectral observables sometimes give pre- and postdenaturation baseline slopes that are nonlinear, and this can complicate thermodynamic analysis. In the present studies on urea- and GdnHCl-induced denaturation of β1, we have assumed pre- and postdenaturation baselines to be linear, and we have left it to the nonlinear least-squares fitting algorithm to determine the slopes and intercepts of the LEM baselines. The parameters shown in Table 1 are the results of such nonlinear least-squares fits to primary data as illustrated in Figures 1, 2, and 4−6.

The problem of having the nonlinear least-squares algorithm resolve the slopes and intercepts of pre- and postdenaturation baselines is that when the predenaturation baseline is quite short (as it is with GdnHCl-induced denaturation of β1), small deviations or irregularities in the baseline of an observable can result in an unreasonable fit of the baseline slope, resulting in a $\Delta G^{\circ}_{N\rightarrow D}$ value that disagrees with that obtained using other observables. In such cases, an operator-assisted choice of baseline, one that can be rationally defended, provides an alternative means of analyis. By way of example, in Figure 1B the predenaturation baseline derived from the nonlinear fitting routine (the dashed line of steepest slope) is unreasonable in that it intersects only one point in the predenaturation concentration range. Taking the operator-selected baseline shown in the figure, the dashed line that bisects all the points in the range of 0−0.5 M GdnHCl, gives a fitted $\Delta G^{\circ}_{N\rightarrow D}$ value (2.77 ± 0.07 kcal/mol) that agrees with the $\Delta G^{\circ}_{N\rightarrow D}$ values obtained using other observables while being distinctly different from the $\Delta G^{\circ}_{N\rightarrow D}$ value (2.31 ± 0.13 kcal/mol) determined by means of the algorithm-selected predenaturation baseline. The LEM results obtained from the algorithm-selected baseline promote the conclusion that GdnHCl-induced β1 denaturation is non two-state, while the operator-selected baseline results are consistent with two-state denaturation (see Table 1). For reasons of consistency, we argue in support of the operator-selected CD baseline because it passes through all the data points in the 0−0.5 M GdnHCl range, as do the predenaturation baselines of the other spectral observables used to monitor GdnHCl-induced denaturation.

It is clear that in defining the effects of GdnHCl much hinges on the predenaturation baseline of β1, and in the case of Figure 1B it is useful to ask why the 222 nm ellipticity of β1 appears to decrease in the 0−0.5 M GdnHCl range. The predenaturation baseline is also at issue when the Stokes radius is used as an observable in monitoring GdnHCl-induced denaturation. The Stokes radius data (Figure 2) provide evidence that the N ensemble expands its dimensions in a hyperbolic manner, changing most markedly over the same 0−0.5 M GdnHCl range as do the observed ellipticity changes. The overall change in 222 nm ellipticity is modest in the 0−0.5 M GdnHCl range, but the fact that the sign of the change is opposite that expected for denaturation suggests it is part of a phenomenon involving only the N state ensemble, the dominant protein species in the 0−0.5 M range. Indeed, the fraction unfolded plot in Figure 2 shows that the [D]/[N] population ratio is hardly changed over the 0−0.5 M range, strongly supporting the conclusion that the Stokes radius and CD changes are reporting on changes in the N state ensemble that occur before onset of the denaturation transition. Additional evidence that GdnHCl can affect the N state ensemble comes from the $\Delta\nu$ experiment conducted at pH 3.5 (Figure 3). As is the case with the Stokes radius, it is seen that, within the 0−0.5 M range, $\Delta\nu$ deviates from the sigmoid behavior expected for the denaturation transition. The result implies that proton uptake ($\Delta\nu$), a thermodynamic parameter (*8*), is reporting a *thermodynamic* change occurring in the N ensemble at the beginning of the N → D transition that is in excess of the thermodynamic shift in N and D populations detected by spectral measurements. There is precedence for this kind of behavior in that the same type of $\Delta\nu$ phenomenon has been observed in greater detail in GdnHCl-induced effects on RNase A (*7*), β-lactoglobulin (*23*), and staphylococcal nuclease (*8*), the latter of which, like β1, has a low $C_{1/2}$ for GdnHCl.

We take the observed deviations in the Stokes radius, $\Delta\nu$, and 222 nm ellipticity in the 0−0.5 M GdnHCl range at pH 3.5 and 5.0 as physical, thermodynamic, and possibly structural evidence of GdnHCl-induced within state changes occurring in the N state ensemble of β1. These within state changes, involving the expansion of the N state ensemble at pH 5 and represented as N → N*, are distinct from the between states thermodynamic shift involving the N to D transition. The major change in the Stokes radius in the predenaturation range occurs between 0 and 0.5 M GdnHCl, a concentration range over which only 1−2% of the N population is converted to D species. These results indicate that the protein undergoes two separable transformations: N → N*, which takes place within the range of 0−0.5 M GdnHCl, and N* → D, which occurs at >0.5 M GdnHCl. We propose that the N → N* conversion is a significant transformation of the N ensemble, with N being both

dimensionally and thermodynamically different from N*. The significance of this thermodynamic change from N to N* is that application of the LEM to the GdnHCl-induced denaturation data results in a $\Delta G^{\circ}_{N\rightarrow D}$ value that represents the thermodynamic stability differences between N* and D, not N and D as is commonly assumed and interpreted. Proteins such as RNase A and β-lactoglobulin that exhibit thermodynamic perturbations of the N state ensemble by GdnHCl similar to that observed with β1 at pH 5 have been classified as protein denaturations that show variable thermodynamic character in the native ensemble outside the transition zone (*8*).

Returning to pH 5 conditions, we find that GdnHCl- and urea-induced denaturations of β1 give different values for $\Delta G^{\circ}_{N\rightarrow D}$ (Figure 6). This behavior is readily understood in light of our proposal that N and N* are thermodynamically distinct species. At pH 5, the within state N $\rightarrow$ N* transformation is completed at a GdnHCl concentration that precedes the between states N* $\rightarrow$ D transition. Thus, LEM analysis of the between states GdnHCl-induced denaturation of β1 reports on the N* $\rightarrow$ D transition while that for urea-induced denaturation reports on the transition involving N $\rightarrow$ D. It follows that if indeed N is thermodynamically different from N*, the two denaturants must give different values for $\Delta G^{\circ}_{N\rightarrow D}$. The results in Figure 7 indicate that increasing salt in the 0−0.8 M range significantly destabilizes β1 with respect to thermal denaturation. Given the observed effects of 0−0.5 M GdnHCl at pH 5 (25 °C) on the Stokes radius of β1 N ensemble, it seems possible that a salt effect of GdnHCl could be responsible for destabilizing the β1 N ensemble, causing the GdnHCl-induced denaturation $\Delta G^{\circ}_{N\rightarrow D}$ value to be less than that determined from urea.

In the context of GdnHCl- and urea-induced protein denaturation, increasing neutral salt concentration has been shown to increase the stability of thioredoxin, RNase T1, RNase A, ubiquitin, and other proteins (*7*, *24*−*27*). By contrast, salt appears to decrease β1 thermal stability up to a concentration of 0.8 M while increasing thermal stability at higher concentrations. Thus, our proposal that the salt effect of GdnHCl in the low concentration range causes a transformation of the N ensemble to a less stable form (N $\rightarrow$ N*) is based on several observations that include the lower value of $\Delta G^{\circ}_{N\rightarrow D}$ obtained for GdnHCl-induced denaturation relative to that obtained from urea, the dimensional changes of the β1 N ensemble that occur over the same GdnHCl concentration range, the negatively sloping 222 nm CD baseline for β1 at predenaturational concentrations of GdnHCl, and the fact that RNase A and β-lactoglobulin exhibit within state thermodynamic effects on their respective native ensembles in the GdnHCl concentration range preceding the major denaturing transition in a manner similar to that of β1 (*8*). Like RNase A and β-lactoglobulin, with GdnHCl-induced denaturation β1 exhibits variable two-state behavior in that the free energy of the native ensemble in the predenaturation zone changes (varies) with GdnHCl concentration in a nonlinear manner. This proposal forms the basis of ongoing studies concerned with a more complete dissection of the effects of denaturants on various states of β1, the implications of the effects on thermodynamic evaluations of stability, and the relationship of denaturant-induced thermodynamic effects to thermally induced denaturation of β1.

Some proteins show identical values of $\Delta G^{\circ}_{N\rightarrow D}$ from application of the LEM using GdnHCl- and urea-induced unfolding (*1*, *3*), but for many protein systems, GdnHCl and urea extrapolate to different $\Delta G^{\circ}_{N\rightarrow D}$ values (*2*, *4*, *6*, *8*, *28*). Several groups have looked into the question of why these differences arise, with some concluding that ionic or salt effects inherent to GdnHCl (but not to urea) play an important role and others indicating that the LEM is applicable to urea but not to GdnHCl (*6*−*8*, *24*, *26*, *29*, *30*). In all cases, there is strong rationale for the conclusion that $\Delta G^{\circ}_{N\rightarrow D}$ obtained from GdnHCl is more prone to inaccuracies and extraneous complexities than $\Delta G^{\circ}_{N\rightarrow D}$ obtained using urea extrapolation. Despite this endorsement of urea-induced unfolding evaluations of $\Delta G^{\circ}_{N\rightarrow D}$, it is likely that GdnHCl-induced unfolding measurements will continue to appear in the literature and conclusions about protein stability drawn from LEM analyses. Our view is that the distinction between within state and between states effects of denaturants on the N and D states of the protein and the development of extra-spectroscopic ways to monitor denaturant-induced effects on proteins provide a relatively direct approach to understanding thermodynamic processes associated with denaturant-induced protein unfolding. The work presented here is the first in a series of papers on β1 providing in-depth investigations of denaturant-derived $\Delta G^{\circ}_{N\rightarrow D}$ values. Our intention is to seek insight into behavior responsible for denaturant-induced effects in order to better define and understand the underlying molecular processes.

ACKNOWLEDGMENT

We thank Dr. Lynne Regan for providing the plasmid construct for β1.

REFERENCES

1. Greene, R. F., and Pace, C. N. (1974) Urea and guanidine hydrochloride denaturation of ribonuclease, lysozyme, α-chymotrypsin, and β-lactoglobulin, *J. Biol. Chem. 249*, 5388−5393.
2. Pace, C. N. (1986) in *Enzyme Structure* (Hirs, C. H. W., and Timasheff, S. N., Eds.) Part L, pp 266−280, Academic Press, New York.
3. Santoro, M. M., and Bolen, D. W. (1988) Unfolding free energy changes determined by the linear extrapolation method. 1. Unfolding of phenylmethanesulfonyl α-chymotrypsin using different denaturants, *Biochemistry 27*, 8063−8068.
4. Pace, C. N., and Vanderburg, K. E. (1979) Determining globular protein stability: Guanidine hydrochloride denaturation of myoglobin, *Biochemistry 18*, 288−292.
5. Pace, C. N. (1975) The stability of globular proteins, *CRC Crit. Rev. Biochem. 3*, 1−43.
6. Monera, O. D., Kay, C. M., and Hodges, R. S. (1994) Protein denaturation with guanidine hydrochloride or urea provides a different estimate of stability depending on the contributions of electrostatic interactions, *Protein Sci. 3*, 1984−1991.
7. Yao, M., and Bolen, D. W. (1995) How valid are denaturant-induced unfolding free energy measurements? Level of conformance to common assumptions over an extended range of ribonuclease A stability, *Biochemistry 34*, 3771−3779.
8. Bolen, D. W., and Yang, M. (2000) Effects of guanidine hydrochloride on the proton inventory of proteins: Implications on interpretations of protein stability, *Biochemistry 39*, 15208−15216.
9. Smith, C. K., Withka, J. M., and Regan, L. (1994) A thermodynamic scale for the beta-sheet forming tendencies of the amino acids, *Biochemistry 33*, 5510−5517.
10. Edelhoch, H. (1967) Spectroscopic determination of tryptophan and tyrosine in proteins, *Biochemistry 6*, 1948−1954.

11. Gill, S. C., and von Hippel, P. H. (1989) Calculation of protein extinction coefficients from amino acid sequence data, *Anal. Biochem. 182*, 319−326.
12. Pace, C. N., Vajdos, F., Fee, L., Grimsley, G., and Gray, T. (1995) How to measure and predict the molar absorption coefficient of a protein, *Protein Sci. 4*, 2411−2423.
13. Savitzky, A., and Golay, M. J. E. (1964) Smoothing and differentiation of data by simplified least squares procedures, *Anal. Chem. 36*, 1627−1639.
14. Ragone, R., Colonna, G., Balestrieri, C., Servillo, L., and Irace, G. (1984) Determination of tyrosine exposure in proteins by second-derivative spectroscopy, *Biochemistry 23*, 1871−1875.
15. Rossotti, F. J. C., and Rossotti, H. (1965) Potentiometric titrations using Gran Plots, *J. Chem. Educ. 42*, 375−378.
16. Uversky, V. N. (1993) Use of fast protein size-exclusion liquid chromatography to study the unfolding of proteins which denature through the molten globule, *Biochemistry 32*, 13288−13298.
17. Corbett, R. J. T., and Roche, R. S. (1984) Use of high-speed size-exclusion chromatography for the study of protein folding and stability, *Biochemistry 23*, 1888−1894.
18. Kawahara, K., and Tanford, C. (1966) Viscosity and density of aqueous solutions of urea and guanidine hydrochloride, *J. Biol. Chem. 241*, 3228−3232.
19. Mazurkiewicz, J., Tomasik, P., and Zaplotny, J. (2001) Relationships between water activity and viscosity of solutions, *Food Hydrocolloids 15*, 43−46.
20. Bolen, D. W., and Santoro, M. M. (1988) Unfolding free energy changes determined by the linear extrapolation method. 2. Incorporation of ΔG°_{N-U} values in a thermodynamic cycle, *Biochemistry 27*, 8069−8074.
21. Huang, Y., and Bolen, D. W. (1993) Covalent bond changes as a driving force in enzyme catalysis, *Biochemistry 32*, 9329−9339.
22. Baskakov, I., and Bolen, D. W. (1998) Monitoring the sizes of denatured ensembles of staphyloccal nuclease proteins: Implications regarding *m* values, intermediates, and thermodynamics, *Biochemistry 37*, 18010−18017.
23. Nozaki, Y., and Tanford, C. (1967) in *Enzyme Structure* (Hirs, C. H. W., Ed.) pp 715−734, Academic Press, New York.
24. Santoro, M. M., and Bolen, D. W. (1992) A test of the linear extrapolation of unfolding free energy changes over an extended denaturant concentration range, *Biochemistry 31*, 4901−4907.
25. Mayr, L. M., and Schmid, F. X. (1993) Stabilization of a protein by guanidinium chloride, *Biochemistry 32*, 7994−7998.
26. Makhatadze, G. I. (1999) Thermodynamics of protein interactions with urea and guanidinium hydrocloride, *J. Phys. Chem. B 103*, 4781−4785.
27. Pace, C. N., and Grimsley, G. R. (1988) Ribonuclease T_1 is stabilized by cation and anion binding, *Biochemistry 27*, 3242−3246.
28. Pace, C. N., Laurents, D. V., and Thomson, J. A. (1990) pH dependence of the urea and guanidine hydrochloride denaturation of ribonuclease A and ribonuclease T1, *Biochemistry 29*, 2564−2572.
29. Dill, K. (1990) Dominant forces in protein folding, *Biochemistry 29*, 7133−7155.
30. Alonso, D., and Dill, K. (1991) Solvent denaturation and stabilization of globular proteins, *Biochemistry 30*, 5974−5985.

BI048666J